J|A|C|S
ARTICLES
Published on Web 04/01/2004

A Comparison of C−F and C−H Bond Activation by Zerovalent Ni and Pt: A Density Functional Study

Meike Reinhold, John E. McGrady,* and Robin N. Perutz*

Contribution from the Department of Chemistry, University of York, Heslington, York YO10 5DD, United Kingdom

Received November 19, 2003; E-mail: jem15@york.ac.uk; rnp1@york.ac.uk

Abstract: Density functional theory indicates that oxidative addition of the C−F and C−H bonds in C_6F_6 and C_6H_6 at zerovalent nickel and platinum fragments, $M(H_2PCH_2CH_2PH_2)$, proceeds via initial exothermic formation of an η^2-coordinated arene complex. Two distinct transition states have been located on the potential energy surface between the η^2-coordinated arene and the oxidative addition product. The first, at relatively low energy, features an η^3-coordinated arene and connects two identical η^2-arene minima, while the second leads to cleavage of the C−X bond. The absence of intermediate C−F or C−H σ complexes observed in other systems is traced to the ability of the 14-electron metal fragment to accommodate the η^3-coordination mode in the first transition state. Oxidative addition of the C−F bond is exothermic at both nickel and platinum, but the barrier is significantly higher for the heavier element as a result of strong 5dπ−pπ repulsions in the transition state. Similar repulsive interactions lead to a relatively long Pt−F bond with a lower stretching frequency in the oxidative addition product. Activation of the C−H bond is, in contrast, exothermic only for the platinum complex. We conclude that the nickel system is better suited to selective C−F bond activation than its platinum analogue for two reasons: the strong thermodynamic preference for C−F over C−H bond activation and the relatively low kinetic barrier.

Introduction

The utility of fragments such as Cp_2W, $CpReL_2$, $CpM(PR_3)$ (M = Rh, Ir), and $[Pt(N{-}N)(CH_3)L]^+$ in the oxidative addition of aromatic carbon−hydrogen bonds has been documented extensively, and many of the electronic requirements for effective bond activation have been rationalized.[1−12] Such fragments form strong metal−carbon and metal−hydrogen bonds, compensating for the strength of the C−H bonds in the starting materials.[3,13] Activation of aromatic carbon−fluorine bonds has now also been observed with a wide variety of transition metals and electron configurations.[14−23] While some systems such as $Cp^*Re(CO)_3$ resemble typical C−H bond activators,[18] others such as Ni(dtbpe) (dtbpe = $^tBu_2PCH_2CH_2P^tBu_2$) and $Ni(PEt_3)_2$ are effective at C−F but not C−H activation.[17,19] If C−F bond activators are to find application, they will almost certainly have to exhibit similar selectivity for C−F over C−H bonds.

(1) Arndtsen, B. A.; Bergman, R. G.; Mobley, T. A.; Peterson, T. H. *Acc. Chem. Res.* **1995**, *28*, 154.
(2) (a) Labinger; J. A.; Bercaw, J. E. *Nature* **2002**, *4171*, 507. (b) Johansson, L.; Tilset, M.; Labinger, J. A.; Bercaw, J. E. *J. Am. Chem. Soc.* **2000**, *122*, 10846.
(3) (a) Jones, W. D. *Top. Organomet. Chem.* **1999**, *3*, 9. (b) Wick, D. D.; Jones, W. D. *Organometallics* **1999**, *18*, 495. (c) Jones, W. D. *Acc. Chem. Res.* **2003**, *36*, 140. (d) Dong, L.; Belt, S. T.; Duckett, S. B.; Partridge, M. G.; Jones, W. D.; Perutz, R. N. *J. Chem. Soc., Chem. Commun.* **1991**, 266. (e) Chin, R. M.; Dong, L.; Duckett, S. B.; Partridge, M. G.; Jones, W. D.; Perutz, R. N. *J. Am. Chem. Soc.* **1993**, *115*, 7685.
(4) Crabtree, R. H. *J. Chem. Soc., Dalton Trans.* **2001**, 2437.
(5) (a) Green, J. C.; Harvey, J. N.; Poli, R. *J. Chem. Soc., Dalton Trans.* **2002**, 1861. (b) Green, J. C. *Chem. Soc. Rev.* **1998**, 263.
(6) (a) Churchill, D. G.; Janak, K. E.; Wittenberg, J. S.; Parkin, G. P. *J. Am. Chem. Soc.* **2003**, *125*, 1403. (b) Janak, K. E.; Parkin G. P. *J. Am. Chem. Soc.* **2003**, *125*, 6889.
(7) Vigalok, A.; Uzan, O.; Shimon, L. J. W.; Ben-David, Y.; Martin, J. M. L.; Milstein, D. *J. Am. Chem. Soc.* **1998**, *120*, 12539.
(8) Johansson, L.; Tilset, M.; Labinger, J. A.; Bercaw, J. E. *J. Am. Chem. Soc.* **2000**, *122*, 10846.
(9) Peterson, T. H.; Golden J. T.; Bergman, R. G. *J. Am. Chem. Soc.* **2001**, *123*, 455.
(10) Reinartz, S.; White, P. S.; Brookhart, M.; Templeton, J. L. *J. Am. Chem. Soc.* **2001**, *123*, 12724; **2002**, *124*, 7249.
(11) Sakaki, S.; Biswas, B.; Sugimoto, M. *Organometallics* **1998**, *17*, 1278.
(12) Heiberg, H.; Swang, O.; Ryan, O. B.; Gropen, O. *J. Phys. Chem. A* **1999**, *103*, 10004.
(13) (a) Clot, E.; Eisenstein O.; Maseras, F.; Megret, C.; Oelckers, B.; Perutz, R. N. *Chem. Commun.* **2003**, 490. (b) Clot, E.; Oelckers, B.; Klahn, H.; Eisenstein, O.; Perutz, R. N. *J. Chem. Soc., Dalton Trans.* **2003**, 4065. (c) Carbo, J. J.; Eisenstein, O.; Higgitt, C. L.; Klahn, H.; Maseras, F.; Oelckers, B.; Perutz, R. N. *J. Chem. Soc., Dalton Trans.* **2001**, 1452.
(14) Tsou, T. T.; Kochi, J. K. *J. Am. Chem. Soc.* **1979**, *101*, 6319.
(15) (a) Burdeniuc, J.; Jedlicka, B.; Crabtree, R. H. *Chem. Ber./Recl.* **1997**, *130*, 145. (b) Kiplinger, J. L.; Richmond, T. G.; Osterberg, C. E. *Chem. Rev.* **1994**, *94*, 373. (c) Murphy, C. E.; Murugavel, R.; Roesky, H. W. *Chem. Rev.* **1997**, *97*, 3425. (d) Richmond, T. G. In *Topics in Organometallic Chemistry*; Murai, S., Ed.; Springer: New York, 1999; Vol. 3, pp 243−269.
(16) Hofmann, P.; Unfried, G. *Chem. Ber.* **1992**, *125*, 659.
(17) Bach, I.; Pörschke, K.-R.; Goddard, R.; Kopiske, C.; Krüger, C.; Rufinska, A.; Seevogel, K. *Organometallics* **1996**, *15*, 4959.
(18) (a) Klahn, A. H.; Moore, M. H.; Perutz, R. N. *J. Chem. Soc., Chem. Commun.* **1992**, 1699. (b) Klahn, A. H.; Oelckers, B.; Godoy, F.; Garland, M. T.; Vega, A.; Perutz, R. N.; Higgitt, C. L. *J. Chem. Soc., Dalton Trans.* **1998**, 3079.
(19) (a) Braun, T.; Perutz, R. N. *Chem. Commun.* **2002**, 2749. (b) Cronin, L.; Higgitt, C. L.; Karch, R.; Perutz, R. N. *Organometallics* **1997**, *16*, 4920. (c) Braun, T.; Foxon, S. P.; Perutz, R. N.; Walton, P. H. *Angew. Chem., Int. Ed.* **1999**, *38*, 3326. (d) Sladek, M. I.; Braun, T.; Neumann, B.; Stammler, H.-G. *Dalton Trans*. **2002**, 297. (e) Braun, T.; Sladek, M. I.; Perutz, R. N. *Chem. Commun.* **2001**, 2254.
(20) Whittlesey, M. K.; Perutz, R. N.; Moore, M. H. *J. Chem. Soc., Chem. Commun.* **1996**, 787.
(21) Kraft, B. M.; Lachicotte, R. J.; Jones, W. D. *J. Am. Chem. Soc.* **2001**, *123*, 10973. Kraft, B. M.; Jones, W. D. *J. Organomet. Chem.* **2002**, *658*, 132.
(22) (a) Aizenberg, M.; Milstein, D. *Science* **1994**, *265*, 359. (b) Aizenberg, M.; Milstein, D. *J. Am. Chem. Soc.* **1995**, *117*, 8674.
(23) Braun, T.; Noveski, D.; Neumann, B.; Stammler, H. G. *Angew. Chem., Int. Ed.* **2002**, *41*, 2745.

10.1021/ja0396908 CCC: $27.50

Scheme 1. Reactivity of Ni(dtbpe)Me_2 with C_6H_6 and C_6F_6 (after ref 17)

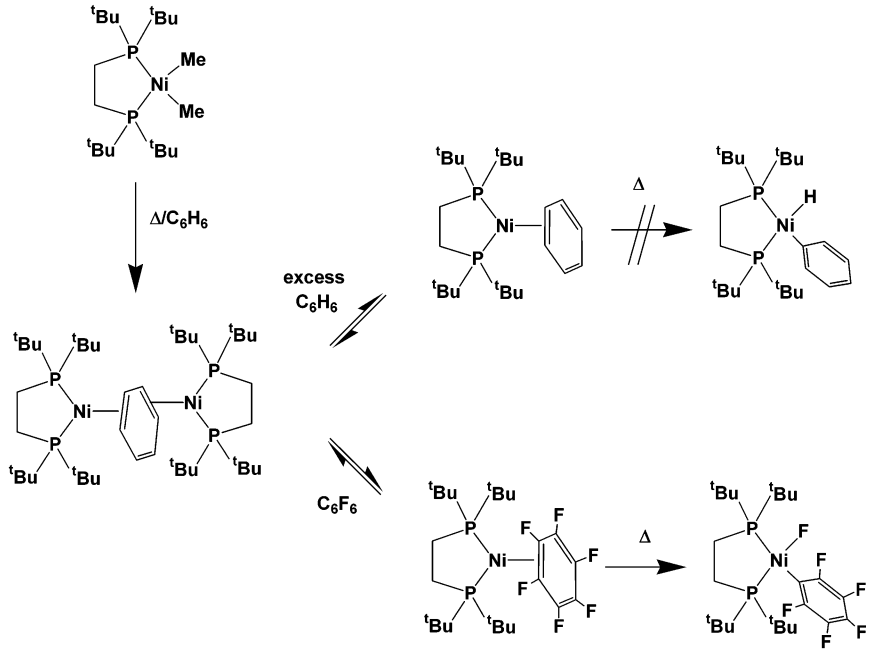

Pörschke and co-workers have described a detailed study of the coordination chemistry of the 14-electron fragment, Ni(dtpbe), with a variety of arenes.[17] This fragment, generated in situ by thermal elimination of ethane from Ni(dtpbe)$(Me)_2$, reacts with benzene to form bimetallic $\{Ni(dtpbe)\}_2(\mu\text{-}\eta^2\text{:}\ \eta^2\text{-}C_6H_6)$. This species is in equilibrium with the 1:1 adduct Ni(dtpbe)$(\eta^2\text{-}C_6H_6)$, which is favored in the presence of a large excess of benzene. Similarly, excess C_6F_6 yields the fluorinated η^2-coordinated complex, Ni(dtpbe)$(\eta^2\text{-}C_6F_6)$. However, of the two η^2-coordinated species, Ni(dtpbe)$(\eta^2\text{-}C_6H_6)$ and Ni(dtpbe)$(\eta^2\text{-}C_6F_6)$, only the latter undergoes thermal oxidative addition, forming Ni(dtpbe)$(C_6F_5)F$ at 293 K (Scheme 1). The corresponding chemistry of $Ni(PEt_3)_2$ was first examined by Fahey and Mahan, who provided circumstantial evidence for oxidative addition of hexafluorobenzene in its reaction with $Ni(COD)_2$ (COD = 1,5-cyclooctadiene) in the presence of PEt_3.[24] A more thorough study by Cronin et. al. documented the oxidative addition and characterized the product *trans*-$Ni(PEt_3)_2(C_6F_5)F$ crystallographically (Scheme 2).[19] The same product was obtained by reaction of $Ni(PEt_3)_4$ in the absence of COD. Although no precursor of the type $Ni(PEt_3)_2(\eta^2\text{-}C_6F_6)$ has been observed, the naphthalene analogue, $Ni(PEt_3)_2(\eta^2\text{-}C_{10}F_8)$, has been characterized and demonstrated to convert to the oxidative addition product, *trans*-$Ni(PEt_3)_2(C_{10}F_7)F$.[25] Cronin et. al. have also shown that C−F oxidative addition occurs in pentafluorobenzene, but no evidence of C−H activation of benzene or partially fluorinated benzenes has been documented. Oxidative addition chemistry at platinum is notably different; Whitesides et al. studied the reaction of benzene with Pt(dcpe) (dcpe = $Cy_2PCH_2CH_2PCy_2$), formed by reductive elimination from Pt(dcpe)(neopentyl)H, and showed that oxidative addition occurred to yield Pt(dcpe)$(C_6H_5)H$ via Pt(dcpe)$(\eta^2\text{-}C_6H_6)$.[26] The reactivity

Scheme 2. Reactivity of $Ni(COD)_2/PEt_3$ with C_6F_6 and $C_{10}F_8$ (after refs 19 and 25)

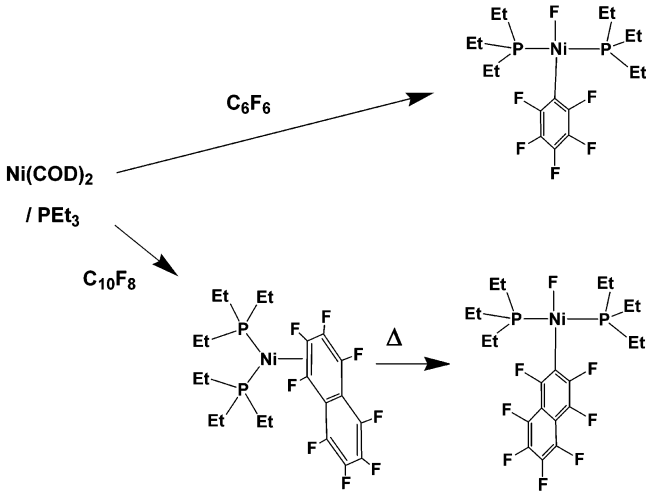

of Pt(dtbpm) (dtbpm = $^tBu_2PCH_2P^tBu_2$) appears to be significantly different from that of Pt(dcpe). It does not undergo C−H activation with benzene but shows interesting reactivity toward 1,4-$C_6H_4(CF_3)_2$. At lower temperatures the η^2-arene complex is formed but at 358 K, C−H activation occurs.[27] The first direct oxidative addition reaction of hexafluorobenzene was that observed by Hofmann at Pt(dtbpm) but no further intermolecular C−F activation chemistry at platinum has been reported.[16] Competition between C−H and C−F activation has barely been tested at platinum, but we note that $Pt(PCy_3)_2$ reacts with pentafluorobenzene to form the C−H activation product, Pt$(PCy_3)_2(C_6F_5)H$, only.[28]

Recent improvements in synthetic routes to metal fluorides have allowed systematic comparisons between these complexes

(24) Fahey, D. R.; Mahan, J. E. *J. Am. Chem. Soc.* **1977**, *99*, 522.
(25) Braun, T.; Cronin, L.; Higgitt, C. L.; McGrady, J. E.; Perutz, R. N.; Reinhold, M. *New J. Chem.* **2001**, *25*, 19.
(26) (a) Hackett, M.; Ibers, J. A.; Whitesides, G. M. *J. Am. Chem. Soc.* **1988**, *110*, 1436. (b) Hackett, M.; Whitesides, G. M. *J. Am. Chem. Soc.* **1988**, *110*, 1449.
(27) Iverson, C. N.; Lachicotte, R. J.; Müller, C.; Jones, W. D. *Organometallics* **2002**, *21*, 5320.
(28) Fornies, J.; Green, M.; Spencer, J. L.; Stone, F. G. A. *J. Chem. Soc., Dalton Trans.* **1977**, 1006.

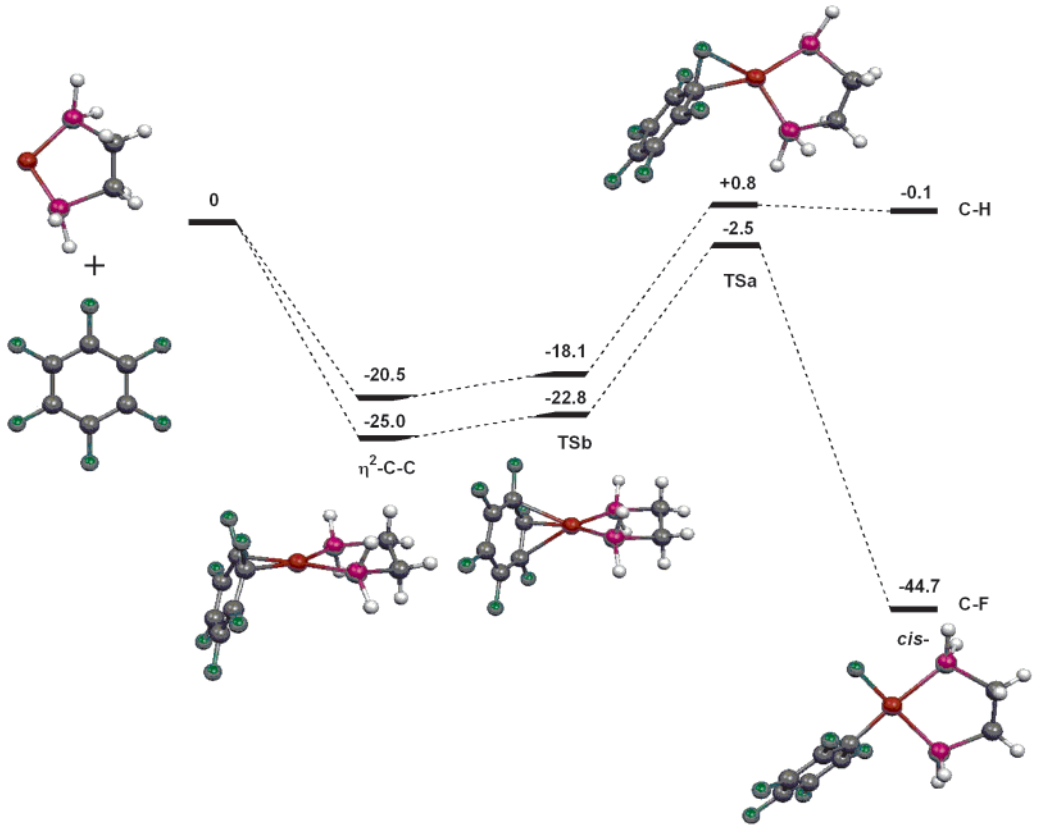

Figure 1. Energetics of C−F and C−H activation by Ni($H_2PCH_2CH_2PH_2$) (energies in kcal mol^{-1}).

and the analogues with the heavier halides. Metal fluorides are acquiring importance in organic fluorination reactions and in secondary interactions especially hydrogen bonding, as well as in C−F bond activation.[29,30] A number of workers who have debated the nature of the M−F bond argue that fluoride is the most effective π-donor of the halides.[31] The interaction between the ligand π orbitals and the metal center (dπ−pπ interactions) is, however, only attractive in the presence of vacant orbitals with appropriate symmetry. In contrast, in square-planar complexes with a d^8 configuration such as those described in this work, the dominant effect is likely to be repulsive unless strong acceptor ligands are also present to induce push−pull effects.[32] The importance of dπ−pπ repulsions in fluoride complexes has, however, been questioned by recent authors who have suggested that the properties of fluoride complexes can be explained instead by the high degree of ionicity in the M−F bond.[33]

In this paper, we use DFT methods to examine the oxidative addition of benzene and hexafluorobenzene to Ni($H_2PCH_2CH_2PH_2$), Ni(PH_3)$_2$, and Pt($H_2PCH_2CH_2PH_2$), which serve as models of the nickel and platinum complexes described above. Our aim is to document the energetics and reaction pathways leading to C−F and C−H oxidative addition and to identify those factors that favor C−F activation. A number of computational studies of C−F activation have emerged in recent years, but these have focused exclusively on second and third row transition metals.[34,35] Here we present the first systematic comparison of the first transition series with third row analogues and show that the former have great potential for selective C−F activation.

Results and Discussion

C−F and C−H Activation by Ni(dtpbe): Thermodynamics and Kinetics. In light of the conspicuously different reactivity of Ni(dtpbe)(η^2-C_6H_6) and Ni(dtpbe)(η^2-C_6F_6), a comparison between the potential energy surfaces for the reaction of Ni($H_2PCH_2CH_2PH_2$) with C_6H_6 and C_6F_6 makes a logical starting point to this study. For the fluorinated system, local minima have been found for both the η^2-coordinated intermediate, Ni($H_2PCH_2CH_2PH_2$)(η^2-C_6F_6), and the product,

(29) (a) Barthazy, P.; Stoop, R. M.; Wörle, M.; Togni, A.; Mezzetti, A. *Organometallics* **2000**, *19*, 2844. (b) Tilset, M.; Hamon, J. R.; Hamon, P. *Chem. Commun.* **1998**, 765. (c) Tilset, M.; Fjeldahl, I.; Hamon, J. R.; Hamon, P.; Toupet, L.; Saillard, J. Y.; Costuas, K.; Haynes, A. *J. Am. Chem. Soc.* **2001**, *123*, 9984. (d) Cooper, A. C.; Bollinger; J. C.; Caulton, K. G. *New J. Chem.* **1998**, *22*, 473. (e) Huang, D.; Koren, P. R.; Folting, K.; Davidson, E. R.; Caulton, K. G. *J. Am. Chem. Soc.* **2000**, *122*, 8916. (f) Fagnou K.; Lautens, M. *Angew. Chem., Int. Ed.* **2002**, *41*, 26. (g) Poulton, J. T.; Sigalas, M. P.; Folting, K.; Streib, W. E.; Eisenstein O.; Caulton, K. G. *Inorg. Chem.* **1994**, *33*, 1476. (h) Jasim, N. A.; Perutz, R. N.; Archibald, S. J. *Dalton Trans.* **2003**, 2184.
(30) (a) Jasim, N. A.; Perutz, R. N. *J. Am. Chem. Soc.* **2000**, *122*, 8685. (b) Jasim, N. A.; Perutz, R. N.; Foxon, S. P.; Walton, P. H. *J. Chem. Soc., Dalton Trans.* **2001**, 1676. (c) Lee, D.-H.; Kown, H. J.; Patel, B. P; Liable-Sands, L. M; Rheingold, A. L.; Crabtree, R. H. *Organometallics* **1999**, *18*, 1615. (d) Brammer, L.; Bruton. E. A.; Sherwood, P. *New J. Chem.* **1999**, *23*, 965. (e) Brammer, L. *Dalton Trans.* **2003**, 3145. (f) Murphy, V. J.; Rabinovitch, D.; Hascall, T.; Klooster, W. T.; Koetzle, T. F.; Parkin, G. *J. Am. Chem. Soc.* **1998**, *120*, 4372. (g) Kirkham, M. S.; Mahon, M. F.; Whittlesey, M. K. *Chem. Commun.* **2001**, 813.
(31) (a) Doherty, N.; Hoffman, N. W. *Chem. Rev.* **1991**, *91*, 553. (b) Grushin, V. V. *Chem. Eur. J.* **2002**, *8*, 1007.
(32) (a) Caulton, K. G. *New J. Chem.* **1994**, *18*, 25. (b) Mayer, J. M. *Comments Inorg. Chem.* **1988**, *8*, 125.
(33) (a) Mezzetti, A.; Becker, C. *Helv. Chim. Acta* **2002**, *85*, 2686. (b) Holland, P. L.; Andersen, R. A.; Bergman, R. G. *Comments Inorg. Chem.* **1999**, *21*, 115.
(34) (a) Su, M.-D.; Chu, S.-Y. *J. Am. Chem. Soc.* **1997**, *119*, 10178. (b) Su, M.-D.; Chu, S.-Y. *J. Am. Chem. Soc.* **1999**, *121*, 1045.
(35) (a) Bosque, R.; Clot, E. Fantacci, S.; Maseras, F.; Eisenstein, O.; Perutz, R. N.; Renkema, K. B.; Caulton, K. G. *J. Am. Chem. Soc.* **1998**, *120*, 12634. (b) Gérard, H.; Davidson, E. R.; Eisenstein, O. *Mol. Phys.* **2002**, *100*, 533. (c) Gérard, H.; Eisenstein, O. *Dalton Trans.* **2003**, 839.

Table 1. Optimized Structures (Interatomic Distances in Å, Angles in deg) and Relative Energies (*E*/kcal mol^{-1}) of Stationary Points on the Ni($H_2PCH_2CH_2PH_2$) + C_6X_6 Potential Energy Surface[a]

	Ni–C[a]	Ni–F[b]	C–C[c]	C–F	Ni–P[d]	Ni–P	P–Ni–P	E
			Ni($H_2PCH_2CH_2PH_2$) + C_6F_6					
Ni($H_2PCH_2CH_2PH_2$)					2.12	2.12	101.3	0
C_6F_6			1.39	1.34				
Ni($H_2PCH_2CH_2PH_2$)(η^2-C_6F_6)	1.97	2.78	1.45	1.37	2.23	2.23	90.1	-25.0
Ni($^tBu_2PCH_2CH_2P^tBu_2$)(η^2-C_6F_6)	(1.94)		(1.49)	(1.38)	(2.23)	(2.23)	(92.2)	
TSb	1.91	2.85	1.43	1.37	2.21	2.21	91.3	-22.8
TSa	2.07	2.05	1.41	1.47	2.28	2.16	91.6	-2.5
Ni($H_2PCH_2CH_2PH_2$)(C_6F_5)F	1.92	1.76	1.39	2.64	2.29	2.21	86.5	-44.7
			Ni($H_2PCH_2CH_2PH_2$) + C_6H_6					
Ni($H_2PCH_2CH_2PH_2$)					2.12	2.12	101.3	0
C_6H_6			1.40	1.09				
Ni($H_2PCH_2CH_2PH_2$)(η^2-C_6H_6)	2.07	2.54	1.43	1.09	2.20	2.20	91.1	-20.5
[Ni($^tBu_2PCH_2CH_2^tBu_2$)]$_2$(μ_2-η^2:η^2-C_6H_6)	(2.01)		(1.42)		(2.16)	(2.16)	(93.9)	
TSb	2.03	2.58	1.42	1.08	2.19	2.19	92.1	-18.1
TSa	1.91	1.46	1.41	1.73	2.22	2.26	88.1	+0.8
Ni($H_2PCH_2CH_2PH_2$)(C_6H_5)H	1.91	1.44	1.41	2.12	2.23	2.27	87.1	-0.1

[a] Pertinent X-ray data are shown in parentheses. [a] Shortest Ni−C distance. [b] Shortest Ni−X distance. [c] C−C bond closest to Ni center. [d] Trans to C.

Ni($H_2PCH_2CH_2PH_2$)(C_6F_5)F. Relative energies of all species are summarized in Figure 1, and optimized structural parameters are collected in Table 1.

The optimized structure of Ni($H_2PCH_2CH_2PH_2$)(η^2-C_6F_6) is typical of η^2-coordinated arenes, and fully consistent with the available crystallographic data. The coordinated C−C bond is substantially lengthened (1.45 vs 1.39 Å in C_6F_6), and there is a distinct folding of the arene ring at the two coordinated carbon centers (angle between the C_6 ring and the coordinated F_2C_2 unit = 148.5°). The Ni−P bond lengths are also somewhat longer than in Ni($H_2PCH_2CH_2PH_2$), reflecting the trans influence of the arene ligand. In the context of the subsequent C−F activation process, it is significant that the C−F bond lengths at the coordinated carbon centers are elongated relative to the free ligand (1.37 vs 1.34 Å) as a result of the reduced conjugation between the fluorine lone pairs and the arene π system. The structure of the C−F activation product is also unremarkable, showing the expected square-planar coordination about the Ni^{II} center. The Ni−P bonds show a distinct asymmetry, the one trans to C_6F_5 being 0.08 Å longer as a result of the stronger trans influence of the pentafluorophenyl group. The calculated total energies indicate that the oxidative addition product is 19.7 kcal mol^{-1} more stable than the η^2-coordinated intermediate, which in turn is 25.0 kcal mol^{-1} more stable than the free reactants.

A transition state (**TSa**) leading to cleavage of the C−F bond has been located at almost exactly the same energy as the free reactants (E = −2.5 kcal mol^{-1}, with a C−F bond length of 1.47 Å, only 0.10 Å longer than that in the η^2-coordinated intermediate). Moreover, the arene ring is oriented such that the sp^2 hybrid orbital on the ipso carbon is involved primarily with bonding to the fluorine center rather than to the nickel (Figure 1). In fact, the transition structure resembles a C−F σ complex, with the C−F bond lying in the P−Ni−P plane to maximize the overlap between the C−F σ* orbital and the HOMO of the metal fragment, the Ni−P σ* orbital (Scheme 3).

A second transition state, **TSb**, has also been located on the potential energy surface, only 2.2 kcal mol^{-1} above the η^2-arene. At this point, the nickel center is coordinated to the ipso carbon (Ni−C = 1.91 Å) and also, rather more weakly, to the two carbon centers in the 2- and 6- positions (Ni−C = 2.31 Å).

Scheme 3. Interaction of C−F Bond with NiP_2 Fragment in **TSa**

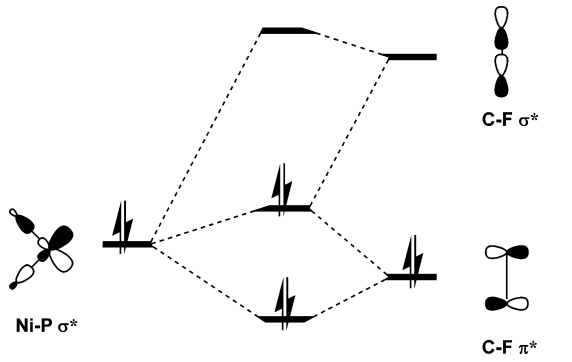

Structurally, **TSb** is therefore very similar to the transition states reported for the ring-hopping motion of $C_6F_2H_4$ at CpRe($CO)_2$,[13c] where the coordination mode of the arene was described as η^3-. A geometry optimization starting from **TSb** confirms that it does indeed connect two equivalent η^2-coordinated arene structures through clockwise and anticlockwise rotations of the ring (Scheme 4). The low barrier to rotation of the C_6F_6 ring is consistent with the observed equivalence of all six F atoms on the NMR time scale even at 188 K (in the ^{t}Bu system).

In a recent study of the reaction of CpRe($CO)_2$ with C_6H_6 by Clot et al.,[13b] a complex very similar in structure to **TSb** was identified as a local minimum, and described as a Re(η^2-C−H) σ complex. All attempts to locate a minimum corresponding to a Ni(η^2-C−F) σ complex on the potential energy surface for Ni($H_2PCH_2CH_2PH_2$)(C_6F_6) (and indeed for all other systems described in this paper) were unsuccessful. This subtle difference between Ni($H_2PCH_2CH_2PH_2$) and CpRe($CO)_2$ can be traced to their valence electron counts, 14 and 16, respectively. In **TSb** the η^3-coordination mode gives a formal valence electron count of 17 for the nickel fragment, but 19 for the rhenium system. The high energy of the η^3-coordinated arene in CpRe($CO)_2$-(C_6H_6) presents a significant barrier between the two equivalent η^2-arene structures (which interconvert only very slowly at room temperature) and also traps the σ complex as a shallow local minimum.

In summary the total reaction coordinate connecting **TSa** with the η^2-arene can be divided into two distinct sections involving

Scheme 4. Schematic Reaction Coordinate, Showing between M(η^2-arene), **TSb** and **TSa**

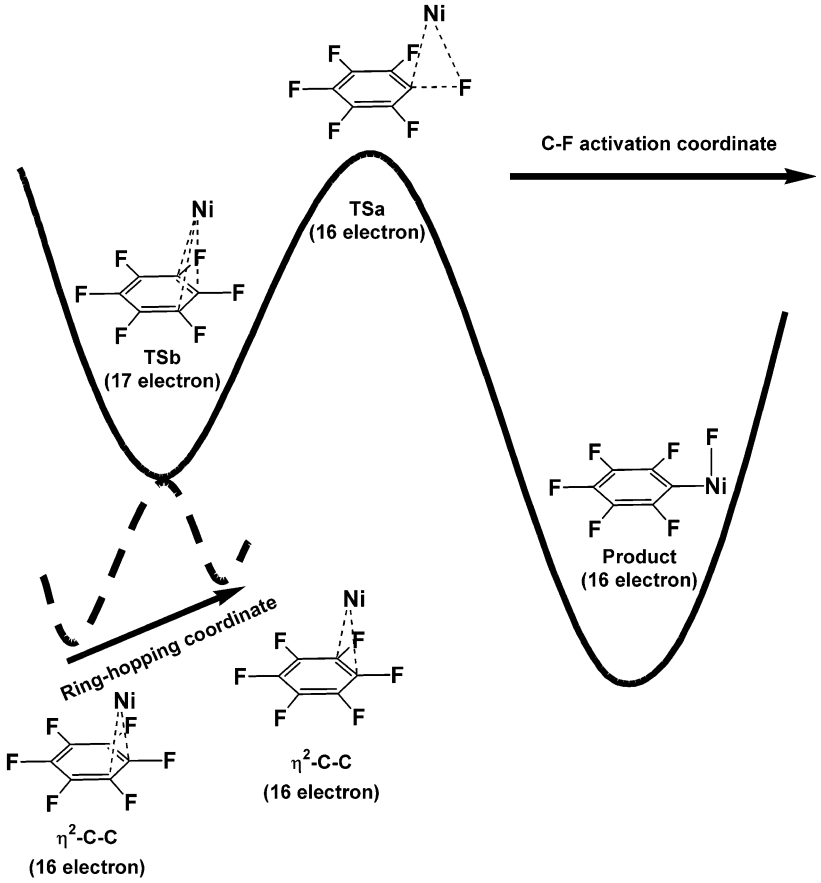

orthogonal internal modes.[36] The first connects **TSa** and **TSb** via a contraction of the C−F bond and migration of the metal to the ipso carbon, while the second connects **TSb** with the η^2-arene structure via a rotation of the ring. (While a transition state generally connects two local minima, a number of cases where it connects a minimum with another transition state have been described.[36]) It is not clear whether the reaction coordinate will pass through **TSb** or go directly from **TSa** to the η^2-arene via a bifurcation point higher on the potential energy surface. What is clear, however, is that there are no secondary minima corresponding to weakly bound σ complexes. The relative energies of the various stationary points are fully consistent with the available experimental data: there is a strong driving force for C−F bond cleavage, but the activation barrier of 22.5 kcal mol^{-1} necessitates thermal activation. The barrier for the reverse reaction, reductive elimination, is 42.2 kcal mol^{-1}, indicating that the reaction will be irreversible. For comparison, an activation barrier of 38.9 kcal mol^{-1} for oxidative addition of a C−F bond was reported by Eisenstein and co-workers for the reaction of C_6F_6 with (Cp)Rh(PH_3),[35] where thermal C−F activation was not observed.

The corresponding stationary points on the potential energy surface for the reaction of Ni($H_2PCH_2CH_2PH_2$) with C_6H_6 are also summarized in Figure 1 and Table 1. They are qualitatively similar to those described for the fluorinated species, but a close inspection of the structural parameters reveals a number of subtle distinctions. In the η^2-coordinated intermediate, Ni(H_2PCH_2-CH_2PH_2)(η^2-C_6H_6), the Ni−C bonds are 0.1 Å longer than those in the corresponding fluorinated species, and the elongation of the coordinated C═C bond and folding of the arene ring (angle between the C_6 ring and the coordinated H_2C_2 unit = 162.3°) are much less pronounced. These trends are fully consistent with experiment and reflect the lower electron-withdrawing ability of the C_6H_6 ring. The weaker back-bonding also results in a lower binding energy (20.5 vs 25.0 kcal mol^{-1} for C_6F_6). The C−H activation product again shows the square planar coordination typical of Ni^{II} species, with the longer Ni−P bond now trans to the more strongly donating hydride ligand. The most striking difference between the two systems, however, lies in the energetics of the oxidative addition step. Cleavage of the C−H bond is strongly endothermic, with the product lying 20.4 kcal mol^{-1} above the η^2-coordinated intermediate. The transition structure for C−H activation (**TSa**) reflects the strong endothermicity of the reaction and is much more product-like than that for the corresponding C−F activation process. Thus the C−H (1.73 Å) and Ni−H (1.46 Å) bonds are almost completely broken and formed, respectively, and the transition state lies only 0.9 kcal mol^{-1} above the products. The absence of a thermodynamic driving force for C−H activation by the nickel system is fully consistent with the experimental observation that only the η^2-arene complex is formed.

As noted in the Introduction, recent work in this group[19] (as well as the earliest attempts at C−F activation by Fahey and Mahan)[24] has focused on complexes with monodentate phosphine ligands rather than the bidentate species described above. A survey of the corresponding potential energy surface using

(36) (a) Bartsch, R. A.; Chae, Y. M.; Ham, S.; Birney, D. M. *J. Am. Chem. Soc.* **2001**, *123*, 7479. (b) Wenthold, P. G.; Hrovat, D. A.; Borden, W. T.; Lineberger, W. C. *Science* **1996**, *272*, 1456.

Table 2. Optimized Structures (Internuclear Separations in Å, Angles in deg) and Relative Energies (*E*/kcal mol^{-1}) of Stationary Points on the Pt($H_2PCH_2CH_2PH_2$) + C_6X_6 Potential Energy Surface

	Pt–C[a]	Pt–F[b]	C–C[c]	C–F	Pt–P[d]	Pt–P	P–Pt–P	E
				Pt($H_2PCH_2CH_2PH_2$) + C_6F_6				
Pt($PH_2CH_2CH_2PH_2$)					2.25	2.25	99.4	0
C_6F_6			1.39	1.34				
Pt($H_2PCH_2CH_2PH_2$)(η^2-C_6F_6)	2.13	2.96	1.47	1.37	2.36	2.36	86.1	-16.4
TSb	2.11	3.01	1.44	1.37	2.31	2.34	88.5	-10.0
TSa	2.24	2.25	1.41	1.55	2.46	2.21	88.5	+12.9
Pt($H_2PCH_2CH_2PH_2$)(C_6F_5)F	2.05	1.98	1.39	2.79	2.36	2.24	85.9	-40.6
				Pt($H_2PCH_2CH_2PH_2$) + C_6H_6				
Pt($H_2PCH_2CH_2PH_2$)					2.25	2.25	99.4	0
C_6H_6			1.40	1.09				
Pt($H_2PCH_2CH_2PH_2$)(η^2-C_6H_6)	2.25	2.71	1.44	1.09	2.33	2.33	88.1	-12.7
TSb	2.32	2.74	1.42	1.08	2.27	2.33	91.5	-7.5
TSa	2.15	1.67	1.41	1.42	2.32	2.39	85.7	+2.8
Pt($H_2PCH_2CH_2PH_2$)(C_6H_5)H	2.06	1.59	1.41	2.47	2.35	2.40	84.2	-12.6

[a] Shortest Pt−C distance. [b] Shortest Pt−X distance. [c] C−C bond closest to Pt center. [d] Trans to C.

$Ni(PH_3)_2$ as the model phosphine (Supplementary data, Figure S1 and Table S1) reveals very similar trends to those shown in Figure 1, except that the both the η^2-arene and the oxidative addition product, *cis*-$Ni(PH_3)_2(C_6F_5)F$, are destabilized by approximately 10 kcal mol^{-1} with respect to free reactants. This difference can be traced to the preference for linear coordination in d^{10} complexes, which can be accommodated in $Ni(PH_3)_2$ but not in $Ni(H_2PCH_2CH_2PH_2)$. Similar destabilization of reactants by chelating ligands, leading to enhanced reactivity, has been extensively discussed by several authors.[11,37]

In the monodentate phosphine system, the final product is *trans*-, rather than *cis*-$Ni(PEt_3)_2(C_6F_5)F$. We have been unable to locate a transition state leading directly to the *trans*-isomer, suggesting that the *cis*-isomer is an intermediate. A number of different pathways can lead to the cis−trans isomerism in square planar complexes, including simple rearrangement via a tetrahedral transition state as well as associative and dissociative mechanisms.[38] We have only explored the simple rearrangement pathway and have located a spin-triplet species $Ni(PH_3)_2(C_6F_5)F$, with approximate tetrahedral geometry, only 5.6 kcal mol^{-1} above the *cis*-isomer. Assuming that the transmission coefficient for crossing from the singlet to the triplet surface approaches unity, the isomerization does not constitute the rate-determining step in the reaction. This is in marked contrast to the C−H activation by $CpRe(CO)_2$, where cis−trans isomerization of the initially formed product was shown to be rate limiting.[13b] Moreover, the low barrier is consistent with the absence of any experimental evidence for the cis isomer as an intermediate.

Comparison of Ni and Pt: Ni($H_2PCH_2CH_2PH_2$) versus Pt($H_2PCH_2CH_2PH_2$). We have previously noted the striking contrast between the oxidative addition chemistry of nickel and platinum. In particular, the 14-electron fragment Pt($Cy_2PCH_2CH_2PCy_2$) has been shown to activate the C−H bond in benzene, whereas the corresponding reaction with Ni(dtpbe) does not occur. In this section we explore reaction pathways for both C−F and C−H activation at the model fragment Pt($H_2PCH_2CH_2PH_2$) and compare the results with those already described for the nickel analogue. Optimized structural parameters for the stationary points are summarized in Table 2, and the reaction pathway is summarized in Figure 2.

The initial step in the reaction again involves exothermic formation of η^2-coordinated arene complexes, although in this case both C_6F_6 and C_6H_6 are bound less strongly (by approximately 8 kcal mol^{-1}) to platinum. As was the case for nickel, replacing the $H_2PCH_2CH_2PH_2$ ligand with two PH_3 units significantly stabilizes the metal fragment, to the extent that neither C_6F_6 nor C_6H_6 binds to $Pt(PH_3)_2$. The trend toward weaker bonding in the platinum congener has been noted in complexes of zerovalent group 10 metals with other neutral ligands (CO, C_2H_4 and C_2H_2).[37e,39]

Turning to the C−F activation process, the oxidative addition remains strongly exothermic, albeit slightly less so than for the corresponding nickel species. The transition state (**TSa**) is, however, significantly higher for platinum (+29.3 kcal mol^{-1}) than for nickel (+22.5 kcal mol^{-1}). A comparison of the structures of the congeneric platinum and nickel species reveals a number of subtle distinctions that relate to the energetics of the process. Most significantly, the difference in length of the M−F bonds (0.22 Å) in M($H_2PCH_2CH_2PH_2$)(C_6F_5)F, is much greater than the difference in either M−C (0.13 Å) or M−P (0.05 Å). The calculated M−F bond lengths are fully consistent with the limited available crystallographic data, which indicate typical Ni^{II}−F and Pt^{II}−F bond lengths in the region of 1.85 Å[19b−d] and 2.04 Å,[40] respectively. We interpret the long Pt−F bonds as indicating substantial repulsion between the fluorine π orbitals and the occupied 5d orbitals of platinum. The reduction of this overlap in the nickel complex is somewhat surprising, given the more compact nature of the 3d orbitals. We note that while π overlap at short separations will undoubtedly be greater for the compact 3d orbitals of nickel, the larger 5d orbitals of platinum give rise to a long-range repulsive "tail". Thus, where overlap is relatively weak, 5dπ−pπ repulsions may be more significant than 3dπ−pπ.

The counterintuitive assertion that dπ−pπ repulsions exert a stronger destabilizing influence in the platinum system has

(37) (a) Hofmann, P.; Perez-Moya, L. A.; Steigelmann, O.; Riede, J. *Organometallics* **1992**, *11*, 1167. (b) Hofmann, P.; Heisee, H.; Neiteler, P.; Müller, G.; Lachmann, J. *Angew. Chem., Int. Ed. Engl.* **1990**, *29*, 880. (c) Simhai, N.; Iverson, C. N.; Edelbach, B. L.; Jones, W. D. *Organometallics* **2001**, *20*, 2759. (d) Zachmanoglou, C. E.; Docrat, A.; Bridgewater, B. M.; Parkin, G.; Brandow, C. G.; Bercaw, J. E.; Jardine, C. N.; Lyall, M.; Green, J. C.; Keister, J. B. *J. Am. Chem. Soc.* **2002**, *124*, 9525. (e) Massera, C.; Frenking, G. *Organometallics* **2003**, *22*, 2758.

(38) (a) Morrell, D. G.; Kochi, J. K. *J. Am. Chem. Soc.* **1975**, *97*, 7262. (b) Tasumi, K.; Nakamura, A.; Komiya, S.; Yamamoto, A.; Yamamoto, T. *J. Am. Chem. Soc.* **1984**, *106*, 8181. (c) Komiya, S.; Albright, T. A.; Hoffmann, R.; Kochi, J. K. *J. Am. Chem. Soc.* **1976**, *98*, 7255.

(39) (a) Liang, B.; Zhou, M.; Andrews, L. *J. Phys. Chem. A* **2000**, *104*, 3905.

(40) (a) Howard, J. A. K.; Woodward, P. *J. Chem. Soc., Dalton Trans.* **1973**, 1840. (b) Russell, D. R.; Mazid, M. A.; Tucker, P. A. *J. Chem. Soc., Dalton Trans.* **1980**, 1737.

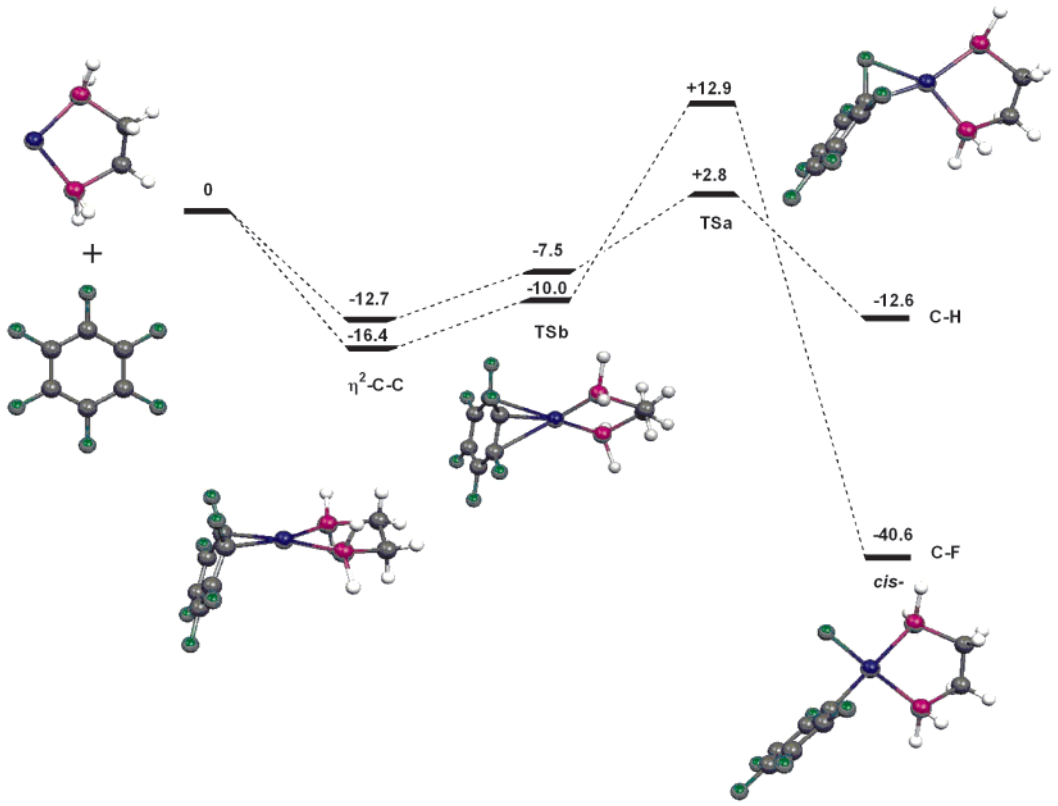

Figure 2. Energetics of C−F and C−H activation by $Pt(H_2PCH_2CH_2PH_2)$ (energies in kcal mol^{-1}).

Scheme 5. Comparison of Energetics of C−F and C−H Activation in Isomeric Products (energies in kcal mol^{-1})

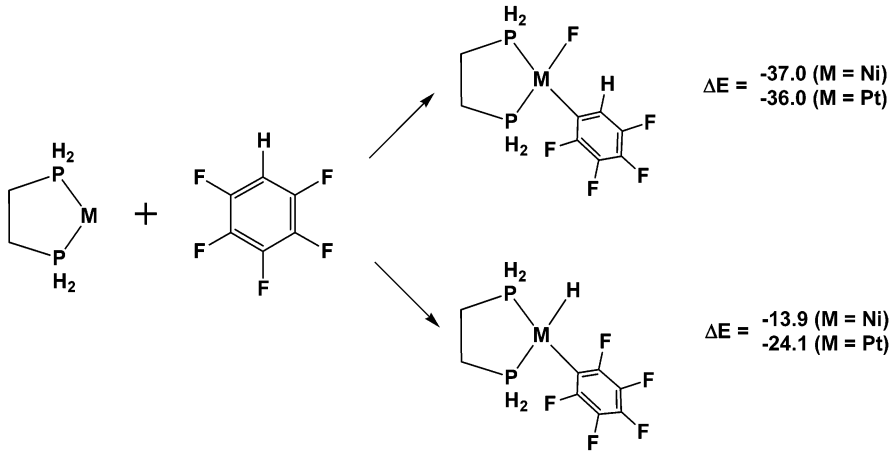

encouraged us to seek further independent measures of the M−F and M−H bond strengths. In a simple computational experiment, we have compared the energetics of C−F and C−H activation processes for the partially fluorinated aromatic C_6F_5H, where the two possible products are isomeric (Scheme 5). Oxidative addition is exothermic (relative to free reactants) in all four cases and, consistent with previous findings,[13] oxidative addition of the C−H bond is more exothermic for C_6F_5H than for C_6H_6. However, activation of the C−F bond is the preferred outcome in these systems, the difference between the two products being 23.1 kcal mol^{-1} and 11.9 kcal mol^{-1} for nickel and platinum, respectively. This clearly indicates that the nickel system shows a stronger preference for C−F activation than platinum. A similar trend can be identified in the hypothetical metathesis reactions shown in Scheme 6, where the two sides of the equation are related by the transfer of fluoride and hydride ligands between nickel and platinum (X = H or F). In both cases (C_6H_5 and C_6F_5), the equilibrium lies to the right, demonstrating the preference for a combination of Ni−F and Pt−H bonds over the Ni−H and Pt−F combination regardless of the identity of the aryl group.

The strengths of the M−F and M−H bonds can be probed independently by calculating vibrational frequencies, which are collected for $M(H_2PCH_2CH_2PH_2)(C_6F_5)F$ and $M(H_2PCH_2CH_2PH_2)(C_6H_5)H$ in Table 3. The data again confirm opposite trends in M−X bond strength; the Pt−H bond is stronger than Ni−H, but Pt−F is weaker than Ni−F. Thus structural, thermodynamic and spectroscopic aspects of our computational results, as well as the available crystallographic data, are consistent with the

Scheme 6. Hypothetical Metathesis Reactions Interchanging Hydride and Fluoride between Ni and Pt (energies in kcal mol^{-1})

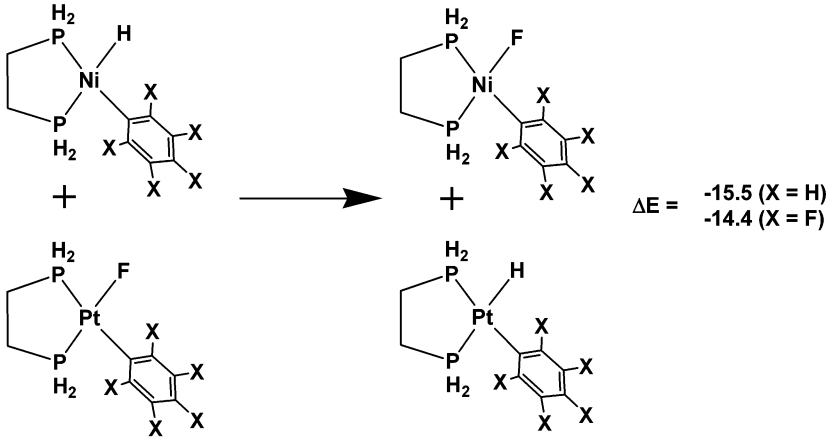

Table 3. Computed Vibrational Frequencies (cm^{-1}) for M−F and M−H Bonds in M($H_2PCH_2CH_2PH_2$)(C_6X_5)X (M = Ni, Pt, X = H, F)

	M = Ni, X = H	M = Ni, X = F	M = Pt, X = H	M = Pt, X = F
ν(M−H)	1948		2095	
ν(M−F)		611, 632, 636[a]		540
ν(M−C)	1044, 1087[b]	1090, 1302[c]	1048, 1097[b]	1097, 1308[c]

[a] Three frequencies have significant Ni−F stretching amplitude, due to coupling to a ring breathing mode of the chelate ring and a torsion about the Ni−C bond. [b] M−C stretch coupled to an in-plane C−H deformation mode. [c] M−C stretch coupled to the C−F (para) stretching mode.

assertion that Pt−F bonds are significantly destabilized relative to their Ni−F counterparts by 5dπ−pπ repulsions.

A comparison of the transition structures for the two species (Tables 1 and 2) suggests that the higher barrier for C−F activation at platinum can also be traced to repulsive dπ−pπ interactions. In particular, while the C−F bond is more elongated in the platinum system, the Pt−C and Pt−F bonds are formed to a far lesser extent. In the transition structure (**TSa**), the occupied metal orbital can interact not only with the vacant C−F σ* orbital, but also with the filled C−F π* (Scheme 3),[35] and the balance of these two interactions (the former stabilizing, the latter destabilizing) will determine the height of the barrier. The increased repulsions between the fluorine lone pairs and the diffuse 5d orbitals in platinum clearly dominate any enhanced overlap with the C−F σ* orbital, leading to relatively long Pt−C and Pt−F bonds and a high activation barrier. Before leaving the comparison of nickel and platinum fluoride systems, we note that the relative strength of the Ni−F bond could also be rationalized in terms of a higher degree of ionicity, as proposed by some groups.[33] However, although the Pauling electronegativities (Ni 1.8, Pt 2.2) predict a more ionic Ni−F bond, the difference between the two metals is marginal. Most importantly, the same trends (viz. elongation of the Pt−F bonds) also emerge in the transition states, where the C−F bond remains largely intact, and hence the incipient M−F bond cannot display significant ionic character. On this basis, we prefer an explanation based on differential dπ-pπ repulsions.

In the corresponding reaction with C_6H_6, the most striking feature of the comparison with nickel is the much greater stability of the platinum C−H activation product, which now lies some 12.6 kcal mol^{-1} below the free reactants. The Pt−H bond clearly does not suffer from dπ−pπ repulsions, and the expansion from nickel to platinum (0.15 Å) is consequently much lower than for M−F bonds and identical to that for the M−C bonds. The greater exothermicity of the C−H activation process leads to a much earlier transition state than in the nickel system, with a less elongated C−H bond (1.42 Å). Moreover, the absence of dπ−pπ repulsions allows a stronger interaction to develop between the metal center and the C−H bond, and the Pt−C bond (2.15 Å) is more fully formed than in the corresponding C−F activation process (2.24 Å). As a result, the transition state is significantly more stable, with a calculated barrier of 15.5 kcal mol^{-1} that is fully consistent with the experimental observation of facile C−H activation at 273 K. Moreover, the activation energy for the reverse reaction, reductive elimination, is only 15.4 kcal mol^{-1} (compared to 53.5 kcal mol^{-1} for the formation of a C−F bond), suggesting that the oxidative addition of a C−H bond will be reversible.

Conclusions

In this paper we have explored the reaction pathways for aromatic C−H and C−F activation at 14-electron, zerovalent nickel and platinum centers. Our calculations indicate that, for both Ni($H_2PCH_2CH_2PH_2$) and Pt($H_2PCH_2CH_2PH_2$), the initial step in the reaction is the exothermic formation of an η^2-coordinated arene complex. In all cases, the complex formed with C_6F_6 is more stable than its C_6H_6 counterpart. The potential energy surface connecting the η^2-arene to the oxidative addition product is a complex one involving two distinct transition states. The metal center first migrates along the C═C bond leading to a transition state (**TSb**) which connects two equivalent η^2-arene structures. From **TSb**, the reaction coordinate follows an orthogonal mode, in which the metal center migrates along the C−X bond, leading to a transition state (**TSa**) where this bond is partially cleaved. The absence of a stable η^2-C−X σ complex on the potential energy surface is associated with the 14-electron configuration of the metal fragment, and distinguishes the reaction pathway from similar process involving 16-electron fragments such as $CpRe(CO)_2$.

For both nickel and platinum, oxidative addition of the C−F bond is strongly exothermic relative to the η^2-arene complex. The kinetic barrier to bond activation is, however, significantly higher for platinum as a result of strong 5dπ−pπ repulsions in the transition state. In marked contrast, C−H bond activation is exothermic only for the platinum system. The accumulated evidence suggests that the switch from nickel to platinum has different effects on M−F and M−H bonds. Whereas the Pt−H

bond benefits from improved overlap compared to nickel, the Pt−F bond is weakened by dπ−pπ repulsions. While other studies have debated the importance of attractive π bonding in metal−fluorine interactions, our studies highlight the role of repulsive π interactions.

In summary, our calculations predict that the nickel complex will show a strong selectivity for C−F over C−H bond activation. For platinum, in contrast, oxidative addition of both aromatic C−H and C−F bonds should be feasible, and C−H and C−F activation should be the kinetic and thermodynamic products, respectively.

Computational Details

All calculations were carried out using the Gaussian 98 program, revision A.7.[41] The B3LYP functional was used throughout,[42] and the nickel and phosphorus atoms were represented by the LANL2 effective core potential and its associated basis set,[43] augmented in the case of phosphorus by a single d polarization function ($\alpha = 0.387$).[44] The 6-31G** basis set was used for all other atoms. Full optimizations were performed without constraint, and vibrational frequencies were calculated to confirm the nature of the stationary points in each case.

Acknowledgment. We are grateful to the University of York and DSM for financial support and Professors Odile Eisenstein and Robert Meier for helpful discussions. We would also like to thank the reviewers for a number of stimulating comments.

Supporting Information Available: Optimized structures (Figure S1) and energies (Table S1) of stationary points for the reaction of $Ni(PH_3)_2 + C_6F_6$ and C_6H_6. Optimized Cartesian coordinates and total energies of the stationary points shown in Tables 1, 2, and S1 and Schemes 5 and 6 (ZIP). This material is available free of charge via the Internet at http://pubs.acs.org.

JA0396908

(41) Frisch, M. J.; Trucks, G. W.; Schlegel, H. B.; Scuseria, G. E.; Robb, M. A.; Cheeseman, J. R.; Zakrzewski, V. G.; Montgomery, J. A.; Stratmann, R. E.; Burant, J. C.; Dapprich, S.; Millam, J. M.; Daniels, A. D.; Kudin, K. N.; Strain, M. C.; Farkas, O.; Tomasi, J.; Barone, V.; Cossi, M.; Cammi, R.; Mennucci, B.; Pomelli, C.; Adamo, C.; Clifford, S.; Ochterski, J.; Petersson, G. A.; Ayala, P. Y.; Cui, Q.; Morokuma, K.; Malick, D. K.; Rabuck, A. D.; Raghavachari, K.; Foresman, J. B.; Cioslowski, J.; Ortiz, J. V.; Stefanov, B. B.; Liu, G.; Liashenko, A.; Piskorz, P.; Komaromi, I.; Gomperts, R.; Martin, R. L.; Fox, D. J.; Keith, T.; Al-Laham, M. A.; Peng, C. Y.; Nanayakkara, A.; Gonzalez, C.; Challacombe, M.; Gill, P. M. W.; Johnson, B. G.; Chen, W.; Wong, M. W.; Andres, J. L.; Head-Gordon, M.; Replogle, E. S.; Pople, J. A. *Gaussian 98*, revisions A.7; Gaussian, Inc.: Pittsburgh, PA, 1998.

(42) (a) Becke, A. D. *Phys. Rev. A* **1988**, *38*, 3098. (b) Lee, C.; Yang, W.; Parr, R. G. *Phys. Rev. B* **1988**, *37*, 785. (c) Becke, A. D. *J. Chem. Phys.* **1993**, *98*, 5648.

(43) Wadt, W. R.; Hay, P. J. *J. Chem. Phys.* **1985**, *82*, 284.

(44) Höllwarth, A.; Böhme, M.; Dapprich, S.; Ehlers, A. W.; Gobbi, A.; Jonas, V.; Köhler, K. F.; Stegmann, R.; Veldkamp, A.; Frenking, G. *Chem. Phys. Lett.* **1993**, *208*, 237.